Inorganic Chemistry

Article

pubs.acs.org/IC

Three Reversible Polymorphic Copper(I) Complexes Triggered by Ligand Conformation: Insights into Polymorphic Crystal Habit and Luminescent Properties

Wenxiang Chai,*[,†,§] Mingwei Hong,[†] Li Song,[‡] Guohua Jia,[†] Hongsheng Shi,[†] Jiayu Guo,[†] Kangying Shu,[†] Bing Guo,[†] Yicheng Zhang,[†] Wenwu You,[∥] and Xueyuan Chen[∥]

[†]College of Materials Science and Engineering, China Jiliang University, Hangzhou 310018, People's Republic of China

[‡]Department of Chemistry, Zhejiang Sci-Tech University, Hangzhou 310018, People's Republic of China

[§]State Key Laboratory of Structural Chemistry and [∥]Key Laboratory of Optoelectronic Materials Chemistry and Physics, Fujian Institute of Research on the Structure of Matter, Chinese Academy of Sciences, Fuzhou 350002, People's Republic of China

Supporting Information

ABSTRACT: Three luminescent polymorphs based on a new copper(I) complex $Cu(2\text{-QBO})(PPh_3)PF_6$ (**1**, PPh_3 = triphenylphosphine, 2-QBO = 2-(2′-quinolyl)benzoxazole) have been synthesized and characterized by FT-IR, UV−vis, elemental analyses, and single-crystal X-ray diffraction analyses. Each polymorph can reversibly convert from one to another through appropriate procedures. Interestingly, such interconversion can be distinguished by their intrinsic crystal morphologies and colors (namely α, dark yellow plate, β, orange block, γ, light yellow needle) as well as photoluminescent (PL) properties. X-ray crystal structure analyses of these three polymorphs show three different supramolecular structures from 1D to 3D, which are expected to be responsible for the formation of three different crystal morphologies such as needle, plate, and block. Combination of the experimental data with DFT calculations on these three polymorphs reveals that the polymorphic interconversion is triggered by the conformation isomerization of the 2-QBO ligand and can be successfully controlled by the polarity of the process solvents (affecting the molecular dipole moment) and thermodynamics (affecting the molecular total energy). It is also found that the different crystal colors of polymorphs and their PL properties are derived from different θ values (dihedral angle between benzoxazolyl and quinolyl group of the 2-QBO ligand) and P−Cu−P angles based on TD-DFT calculations. Moreover, an interesting phase interconversion between γ and β has also been found under different temperature, and this result is consistent with the DFT calculations in which the total energy of β is larger than that of γ. This polymorphism provides a good model to study the relationship between the structure and the physical properties in luminescent copper(I) complexes as well as some profound insights into their PL properties.

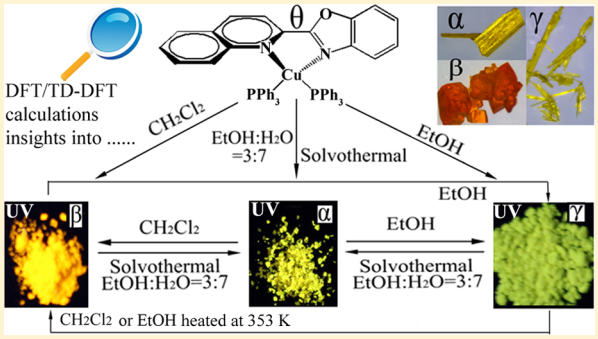

1. INTRODUCTION

In recent years, polymorphism in chemistry has being changed from a "strange and unusual phenomenon" to an interesting and emerging research area.[1] Chemists have employed a variety of unique and efficient approaches to study polymorphism in order to elucidate the relationship between structures and properties of solid state materials.[1] Because of their intrinsic interests, the polymorphism of inorganic compounds and minerals has been extensively studied by geologists and inorganic chemists. Besides the inorganic polymorphism, organic polymorphism has also received considerable attention due to its potential applications in drugs, dyes, etc.[1,2] To date, much more efforts have been done for exploring the relationship between structures and properties of organic polymorphs.[1,2] Also, many types of polymorphism such as supramolecular and conformational polymorphs have been found in organic compounds,[3] including some pseudopolymorphs of hydrate, solvate, and cocrystal.[4] However, rare investigations have been focused on metal−organic compounds, and the associated knowledge of polymorphism in this area is still scattered among the limited literature.[1,2,5] The polymorphism in metal−organic compounds is of significant importance because of its diverse effects on the physicochemical properties of the materials and many consequently important applications.[1,5a] For example, Alq_3 is well known as a good green emitter for organic light-emitting devices (OLEDs) as demonstrated by Tang and co-workers.[6] However, to date, up to five polymorphs of Alq_3 have been found, and they exhibit different emission and electronic transportation properties which are very vital for the device performance of OLEDs.[7] With the bourgeoning interest in highly efficient

Received: November 11, 2014
Published: April 16, 2015

DOI: 10.1021/ic502709b
Inorg. Chem. 2015, 54, 4200−4207

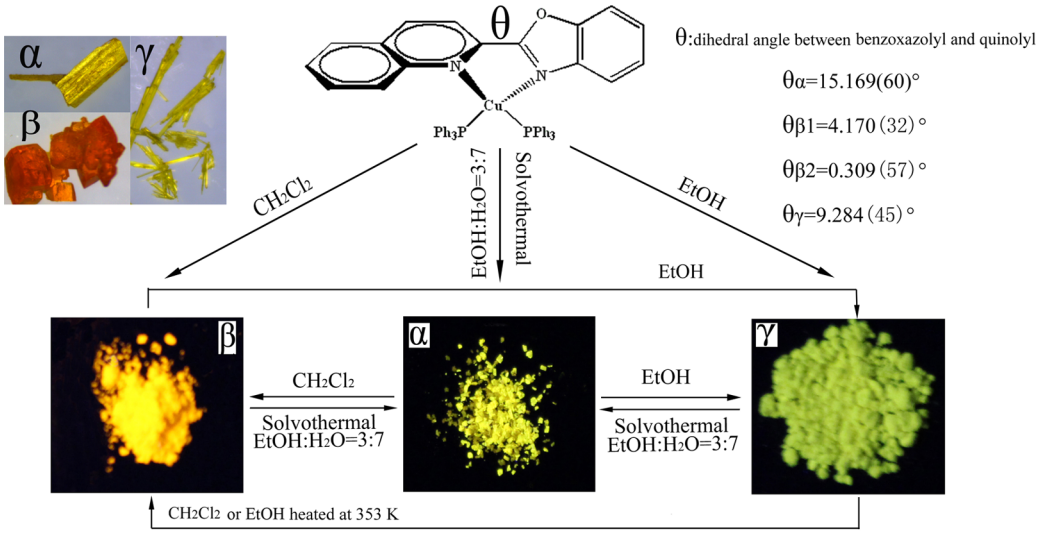

Figure 1. Structural parameters, reversible polymorphic interconversion processes, and corresponding images of three polymorphs.

OLEDs, employing the inexpensive and nontoxic copper(I) complexes as electrophosphorescent materials is becoming very attractive considering that current organically phosphorescent compounds are mainly limited to the third-row noble Ir(III), Pt(II), and Os(II) complexes.[8] Nevertheless, investigations on the polymorphism in this area are still rare. Therefore, full understanding of the polymorphism in the copper(I) complexes is very impendent. To the best of our knowledge, there are only a few reports on the polymorphism of the copper(I) complexes such as two polymorphic luminescent homoligand complexes.[5d] Besides, there is one cuprous iodide cluster,[5f] one cuprous iodide cluster,[5g] and another two cuprous iodide clusters which have been previously reported.[5c]

In this study, we synthesized and characterized three polymorphs of a new luminescent copper(I)−triphenylphosphine complex, Cu(2-QBO)(PPh_3)PF_6 (**1**), bearing a bidentate N-heterocyclic ligand 2-QBO (2-QBO = 2-(2′-quinolyl)-benzoxazole). These three polymorphs (namely, α, dark yellow plate, β, orange block, γ, light yellow needle) can be easily distinguished from one to another not only through their crystalline morphology and color under natural light but also through their PL emission under UV light excitation. With the control of the polarity of the recrystallization solvents and temperature, α, β, and γ polymorphs can reversibly convert from one to another through appropriate procedures (Figure 1). In these conversions, the dihedral angle between the quinolyl ring and the benzoxazole ring of the 2-QBO ligand has an observable change, which is believed to lead to consequent diversities in total system energy (E_T) and physicochemical properties, such as dipole moment (μ), electronic absorption, and PL characteristics. Notably, we found that E_T and μ are two key factors for polymorphic interconversion.

2. EXPERIMENTAL SECTION

2.1. Materials and General Methods. All reagents were purchased as analytical grade and used as received, except that the ligand 2-(2′-quinolyl)benzoxazole (2-QBO) was synthesized according to a literature method reported previously.[9] All solvents were commercially available and used without additional purification. The solvothermal reaction was performed by using a 25 mL Teflon-line stainless steel autoclave under autogenous pressure to grow crystals for single-crystal X-ray diffraction. The infrared spectrum was measured with a Bruker Tensor27 FT-IR spectrophotometer in the range of 4000−400 cm^{-1} in a KBr lamella. Elemental analyses for C, H, and N were performed on an Elementar Vario MICRO analytic instrument. ^1H NMR spectra were obtained with a Bruker Avance II DMX 400 MHz spectrometer. The powder X-ray diffraction (PXRD) data were collected by a Bruker D2 Phaser X-ray diffractometer (Cu Kα, λ = 1.54184 Å). The UV−vis absorption/diffuse reflection spectrum and fluorescence spectrum measurements were performed on a Shimadzu UV3600 spectrometer and a Horiba Jobin-Yvon FL3-211-P spectrometer at room temperature, respectively. For low-temperature measurements, the emission spectra were measured with an Edinburgh Instrument FLS920 spectrometer equipped with continuous (450 W) xenon (Xe) lamps. The samples were mounted on a closed cycle cryostat (10-350 K, DE202, Advanced Research Systems). The line intensities and positions of the measured spectra were calibrated according to the FLS920 correction curve and a standard mercury lamp. TGA-DSC curves were obtained in a static high-purity argon atmosphere with a Mettler Toledo Simultaneous Thermal Analyzer at a heating rate of 10 K/min.

2.2. Synthesis. *[Cu(2-QBO)(PPh_3)$_2$]PF_6 (α Phase).* A mixture of 2-(2′-quinolyl)benzoxazole (2-QBO) (0.1 mmol, 24.6 mg) and triphenylphosphine (PPh_3) (0.2 mmol, 52.5 mg) (in a molar ratio of 1:2) was put into a reaction kettle with EtOH (3 mL) and distilled water (7 mL) in a ratio of 3:7. Then [Cu(MeCN)$_4$]PF_6 (0.1 mmol, 37.3 mg) was added into the mixed slurry. The final mixture was heated to 383 K, kept at this temperature for 3 days, and then cooled down to ambient temperature slowly with a duration of about 3 days. α-Phase yellow plate crystals were obtained. Yield: 72.1 mg, 63%. Mp: 503 K. IR (KBr, cm^{-1}): 3070 (w), 3050 (w), 1500 (w), 1476 (w), 1432 (ms), 1376 (w), 1245 (w), 1145 (w), 1090 (ms), 843 (vs), 744 (s), 692 (s), 557 (ms), 505 (ms). Anal. Calcd: C, 63.77; H, 4.12; N, 2.86. Found: C, 63.60; H, 4.22; N, 2.64.

[Cu(2-QBO)(PPh_3)$_2$]PF_6 (β Phase). A mixture of [Cu(MeCN)$_4$]PF_6 (0.1 mmol, 37.3 mg), 2-(2′-quinolyl)benzoxazole (2-QBO) (0.1 mmol, 24.6 mg), and triphenylphosphine (PPh_3) (0.2 mmol, 52.5 mg) (in a molar ratio of 1:1:2) was stirred in CH_2Cl_2 (10 mL) for 1 h at room temperature. Then the final solution was quickly evaporated at 313 K to obtain a mass of orange crystallite powder to pruduce β phase. Yield: 98.4 mg, 86%. Mp: 503 K. ^1H NMR (400 MHz, $CDCl_3$): δ = 8.79 (d, 1 H), 8.41 (d, 1 H), 8.08 (d, 1 H), 7.93 (d, 1 H), 7.78 (d, 1 H), 7.67 (t, 1 H), 7.54 (t, 1 H), 7.45 (t, 1 H), 7.36 (t s, 7 H), 7.10−7.18 (m s, 25 H) ppm. IR (KBr, cm^{-1}): 3070 (w), 3052 (w), 1500 (vw), 1480 (w), 1435 (ms), 1376 (w), 1245 (w), 1145 (w), 1093 (ms), 840 (vs), 748 (s), 693 (s), 556 (ms), 523 (ms). Anal. Calcd: C, 63.77; H, 4.12; N, 2.86. Found: C, 63.58; H, 4.17; N, 2.65. The orange block crystals appropriate for X-ray structural analysis were obtained from a CH_2Cl_2 solution by covering a layer of EtOH.

DOI: 10.1021/ic502709b
Inorg. Chem. 2015, 54, 4200−4207

Table 1. Crystal Data and Refinement Parameters of α, β, and γ

	α	β	γ
empirical formula	$C_{52}H_{40}N_2O_1P_3F_6Cu$	$C_{52}H_{40}N_2O_1P_3F_6Cu$	$C_{52}H_{40}N_2O_1P_3F_6Cu$
fw	979.31	979.31	979.31
cryst syst	monoclinic	monoclinic	monoclinic
space group	$P2_1/c$	$P2_1/c$	$P2_1/c$
cryst habit	dark yellow plate	orange block	light yellow needle
cryst size(mm)	0.40 × 0.32 × 0.26	0.38 × 0.29 × 0.23	0.32 × 0.26 × 0.20
a (Å)	11.7310(5)	11.0462(4)	14.6421(4)
b (Å)	35.0321(13)	30.5471(12)	15.3930(4)
c (Å)	11.4006(6)	13.9069(2)	20.1585(6)
α (deg)	90	90	90
β (deg)	98.190(4)	99.544(4)	98.680(3)
γ (deg)	90	90	90
V (Å^3)	4637.4(4)	4627.6(3)	4491(2)
Z	4	4	4
D_{calcd} (Mg m^{-3})	1.403	1.406	1.448
μ (mm^{-1})	0.639	0.641	0.660
data/restraints/params	8138/0/586	9074/829/813	7895/0/586
R_{int}	0.0352	0.0409	0.0343
final R indices [$I > 2\sigma(I)$]	R_1 = 0.0552	R_1 = 0.0635	R_1 = 0.0363
	wR_2 = 0.1435	wR_2 = 0.1097	wR_2 = 0.0773
R indices (all data)	R_1 = 0.0770	R_1 = 0.0900	R_1 = 0.0577
	wR_2 = 0.1571	wR_2 = 0.1181	wR_2 = 0.0845
goodness-of-fit on F^2	1.042	1.239	0.992
largest diff. peak and hole (eÅ^{-3})	0.83	0.36	0.38
	−0.38	−0.34	−0.33

Table 2. Calculated Total Energies (E_T) and Dipole Moments (μ) of the System; Energies of HOMO and LUMO Orbitals and HOMO−LUMO Gap (HLG) at the B3LYP/LACVP* Level for α, β, and γ

polymorph	E_T (au)	μ (D)	E_{HOMO} (au)	E_{LUMO} (au)	HLG (eV)
α	−2398.58499960	2.7803	−0.29668	−0.17606	3.2877
β1	−2398.80839592	2.4234	−0.29200	−0.17980	3.0531
β2	−2398.79927889	2.4656	−0.29237	−0.18128	3.0229
γ	−2398.81158167	2.7582	−0.29966	−0.17543	3.3805

[Cu(2-QBO)(PPh$_3$)$_2$]PF$_6$ (γ Phase). A mixture of [Cu(MeCN)$_4$]PF$_6$ (0.1 mmol, 37.3 mg), 2-(2′-quinolyl)benzoxazole (2-QBO) (0.1 mmol, 24.6 mg), and triphenylphosphine (PPh$_3$) (0.2 mmol, 52.5 mg) (in a molar ratio of 1:1:2) was stirred in EtOH (15 mL) for 1 h at room temperature. γ-Phase quickly formed as a pale yellow precipitate. After filtrating and washing with EtOH, γ-phase pale yellow crystallite powder was obtained. Yield: 89.2 mg, 78%. Mp: 503 K. ^{1}H NMR (400 MHz, CD$_3$OD): δ = 8.81 (d, 1 H), 8.44 (d, 1 H), 8.12 (d, 1 H), 8.05 (d, 1 H), 7.86 (d, 1 H), 7.72 (t, 1 H), 7.59 (q, 2 H), 7.46 (t, 1 H), 7.39 (t s, 7 H), 7.16−7.23 (m s, 24 H) ppm. IR (KBr, cm^{-1}): 3070 (w), 3053 (w), 1500 (w), 1478 (w), 1435 (ms), 1374 (w), 1246 (w), 1146 (w), 1094 (ms), 839 (vs), 742 (s), 693 (s), 559 (ms), 510 (ms). Anal. Calcd: C, 63.77; H, 4.12; N, 2.86. Found: C, 63.55; H, 4.21; N, 2.70. The light yellow needle-like crystals appropriate for X-ray structural analysis were obtained by a slow evaporation method from EtOH solution.

2.3. X-ray Crystal Structure Determination. Suitable single crystals of α, β, and γ were selected for X-ray diffraction analyses. Data collections were all performed at 293(2) K on an Oxford Xcalibur (Atlas Gemini ultra) diffractometer with graphite-monochromated Mo Kα radiation (λ = 0.71070 Å) using the ω-scan technique. The structures were solved by the direct method and refined by full-matrix least-squares on F^2 using the SHELXL-97 package.[10] Anisotropic displacement parameters were applied to all non-hydrogen atoms, and organic hydrogen atoms were generated geometrically (C−H = 0.96 Å). Selected bond lengths and angle parameters are collected in Table 1 for all polymorphs. All parameters of hydrogen-bonding interactions for the three polymorphs are gathered in the Supporting Information, Table S1.

2.4. Theoretical Calculations. The calculations described here were carried out using the Gaussian 09 suite of programs.[11] The single-point energy calculations in the ground state (S_0) were performed on the X-ray structures of the three polymorphs using the density functional theory (DFT) method with a three-parameter hybrid functional B3LYP and the LACVP* basis set,[8d] which is a combination basis set including the relativistic effective core potential standard basis set LANL2DZ for Cu and P and the standard 6-31G* basis set for C, H, O, and N. A polarization function was also added for P, i.e., P (ξ(d) = 0.34).[8d] The total energies (E_T) and dipole moments (μ) of the system and energies of the HOMO and LUMO orbitals and HOMO−LUMO gap (HLG) for α, β, and γ are summarized in Table 2. To obtain the components of excited states and the estimates of the vertical electron excitation energies, which include some account of the electron correction, time-dependent DFT (TD-DFT) calculations were also performed on the X-ray structures of the three polymorphs using the same B3LYP method and LACVP* basis set.[8d] The excitation energies, oscillator strength parameters, and corresponding major orbital contributions for the low-lying energy electronic transitions are gathered in Table S2 (Supporting Information) for the three polymorphs.

3. RESULTS AND DISCUSSION

3.1. Synthesis. Three polymorphs were prepared by reacting [Cu(MeCN)$_4$]PF$_6$ with ligands 2-QBO and PPh$_3$ in a 1:1:2 ratio in different solvents and by diverse crystallization

DOI: 10.1021/ic502709b
Inorg. Chem. 2015, 54, 4200−4207

procedures (α, solvothermal synthesis with mixed solvent EtOH/H_2O in volume ratio 3:7; β, rapid evaporation from CH_2Cl_2 solution; γ, precipitation from EtOH solution). All of the polymorphs have been characterized by single-crystal X-ray diffraction analyses. Due to the disorder of the 2-QBO ligand, β phase is treated by a split mode into two parts named β1 and β2. Polymorphs are featured as three similarly tetrahedral complexes with the same space group. What is interesting is their easily achievable reversible interconversion. By employing appropriate recrystallization procedures, any two of them can convert to each other (Figure 1). Obviously, the process solvent must play a vital role in polymorphic formation.[5d,12] In addition, other factors in crystallization such as the temperature should also have some impact on the isomerization, as we observed that β phase mixed with some γ phase was obtained from CH_2Cl_2 solution by slow evaporation, whereas only β phase was obtained from EtOH after quickly evaporating at 353 K, and only γ phase was obtained from EtOH/H_2O mixed solvent at room temperature. These results suggest that γ phase tends to crystallize at a relatively low temperature, whereas a higher temperature favors the formation of β and α phases. In order to clearly understand the formation of the three polymorphs, density functional theory (DFT) calculations were performed on the three X-ray structures on the B3LYP/LACVP* level of theory. The total energy and dipole moment (μ) of each polymorph are listed in Table 2. It is found that γ is the most stable phase with a lower energy of 0.2107 eV than that of β, while α is a metastable phase with a higher energy of 5.9549 eV than that of γ. That is why α can only be synthesized through a solvothermal method. On the other hand, a sequence of α (2.7803D) > γ (2.7582D) > β (2.4445D) is found in the μ values, in accordance with the polarity sequence of the processing solvent in crystallization experiments, indicating that a larger polarity solvent produces a larger μ polymorph. The polarity parameter of E_T^N values of H_2O, EtOH, and CH_2Cl_2 are 1, 0.654, and 0.309, respectively.[13] Some further experiments have also been performed to verify the solvent effect. Similar to EtOH, methanol (0.762), 2-propanol (0.546), and 1-butanol (0.586) convert β to γ. On the contrary, solvents with weaker polarity like chloroform (0.259) or acetonitrile (0.46) convert γ to β in minutes, as expected.

Furthermore, in order to confirm that the interconversion is controlled by the employed solvent in solution, the UV−vis electronic absorption and ^{1}H NMR spectra for the samples of β and γ were measured in corresponding solvents. These spectra for α cannot be measured successfully because of its poor solubility. From UV−vis spectra (Supporting Information, Figure S1) of the solutions, obvious differences can be found between the spectra of β in CH_2Cl_2 and that of γ in EtOH, meaning that two polymorphs appear as two isomerized molecules in solution. When the solvents are exchanged, their spectra also exchange as expected. Thus, β converts to γ in EtOH so that only the characteristic absorption from γ can be observed. In addition, γ converts to β in CH_2Cl_2 so that only the β characteristic absorption is present. Similarly, the solvent-controlled isomerization can also be observed from the ^{1}H NMR spectra. As shown in Figure 2, two spectra of β and γ present a sequence of distinguishable peak shifts, which further demonstrates the isomerized molecules occurring in two solutions. The solvent-exchange experiments have also been done for the ^{1}H NMR spectra (Supporting Information, Figure S2−S3), which clearly indicate that β converts to γ in CD_3OD and γ converts to β in $CDCl_3$.

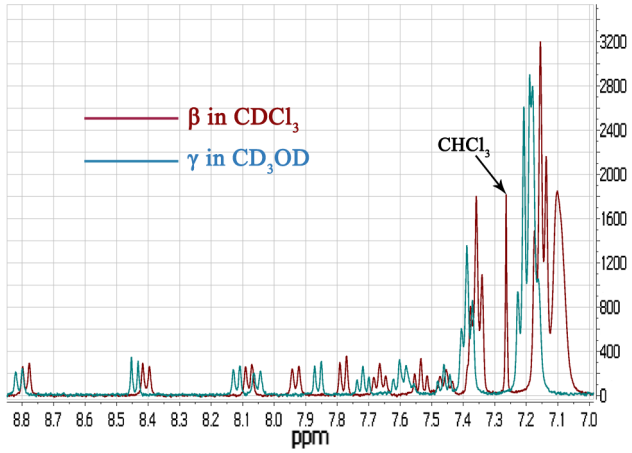

Figure 2. Comparison of ^{1}H NMR spectra for the samples of β in $CDCl_3$ and γ in CD_3OD.

3.2. Crystal Structures. The crystal structures of α, β, and γ are shown in Figure 3. They present a significantly similar

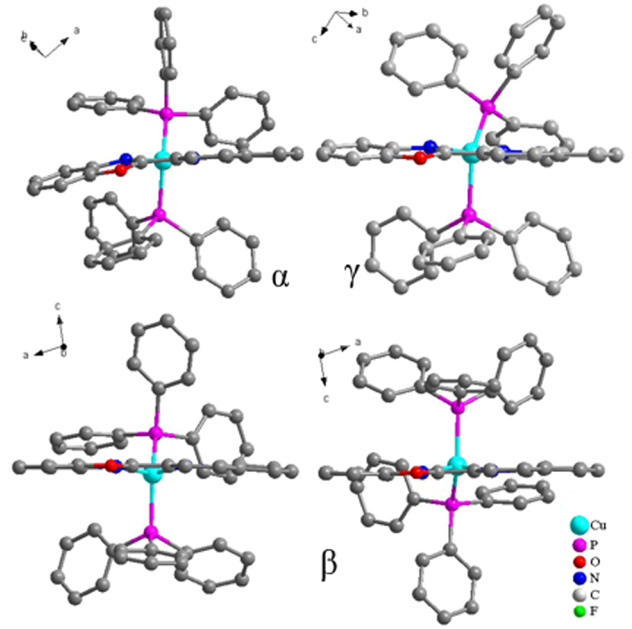

Figure 3. Cationic structures of $[Cu(2\text{-QBO})(PPh_3)_2]PF_6$ complex as three polymorphs. H atoms are omitted for clarity.

distorted tetrahedral configuration around the Cu(I) center constructed by two N atoms from 2-QBO and two P atoms from two PPh_3, which is typical for mononuclear copper(I) complexes.[14] The comparison of the three cationic species reveals an obvious difference in the dihedral angle (θ) between benzoxazolyl and the quinolyl group of the 2-QBO ligand. In α phase, the entire 2-QBO ligand presents an obvious flip with the θ value being 15.169(60)°, while the angles of the other two phases are 4.170(32)° (β1), 0.309(57)° (β2), and 9.284(45)° (γ), showing a sequence of α > γ > β. Klyuev and co-workers previously suggested that the magnitude of the θ value may depend on the temperature and polarity of the solvent.[9] In this case, the magnitude of the θ value is strongly associated with the employed temperature and the polarity of the processing solvent (E_T^N). Thus, a mechanism can be proposed that the changes of the temperature and E_T^N value lead

DOI: 10.1021/ic502709b
Inorg. Chem. 2015, 54, 4200−4207

to the conformational isomerism of 2-QBO and, consequently, result in the formation of three isomeric complexes with variable E_T, μ, and tetrahedral coordination geometry. Notably, the conformational isomerism of 2-QBO should be the key factor in the structure construction which efficiently triggers the interconversion among the three polymorphs.

As shown in Table 3, the Cu−N and Cu−P bond lengths and N−Cu−N and P−Cu−P bond angles are in the normal range,[5b,15] but some differences can also be found, e.g., there is an observed sequence of γ (130.65(2)°) > α (129.03(4)°) > β (127.40(4)°) in the P−Cu−P bond angle. Due to these variations of the cationic species, their packing diagrams also change a lot accordingly. In the α phase, a head-to-head configuration with strong $\pi-\pi$ stacking interaction can be found between the adjacent molecules.[16] In detail, two quinoline rings are parallel with an interplanar spacing as 3.46373(13) Å, centroid to centroid distance as 4.50489(14) Å, and plane to plane shift as 2.88039(18) Å. In addition, a couple of C−H···F hydrogen bonds[17] (C8−H8···F3, 3.212 Å; C38−H38···F3, 3.379 Å) between neighboring molecules also exist, linking the molecules to form a 2D layer structure along the *bc* plane with the collaboration of the $\pi-\pi$ stacking interaction (Supporting Information, Figure S4). Also, this supramolecular structure should be responsible for the plate presentation of its crystal morphology. In the β phase, an alternative stacking array of the intra/intermolecular 2-QBO and phenyl planes can be found with a weak $\pi-\pi$ stacking interaction (intersection angle ≈ 10.325° and centroid to centroid distance ≈ 3.361 Å), forming a supramolecular zigzag chain along the *c* axis. Among all of these chains, strong $\pi-\pi$ stacking interactions between any two of the neighboring 2-QBO can also be observed with almost parallel fashion (dihedral angle being 0.60194(3)°) and small interplanar spacing (~3.423 Å). Thus, all chains are fused together to form a supramolecular wave-like layer along the *ac* plane. Furthermore, a couple of C−H···F hydrogen bonds[17] (C12−H12···F5, 3.191 Å; C45−H45···F5, 3.345 Å) between neighboring wave-like layers are also found, constructing a supramolecular 3D framework structure (Supporting Information, Figure S5). Also, this structure should also be responsible for its crystal morphology (block). Being different from both α and β, no obvious $\pi-\pi$ stacking interaction is found in γ. However, two hydrogen bonds connect the molecules to form a 1D chain along the *a* axis (Supporting Information, Figure S6). Thus, the crystal with a needle morphology is present based on this 1D structure.

Table 3. Selected Bond Lengths (Angstroms) and Angles (degrees) for α, β and, γ

	α	β	γ
Cu(1)−N(1)	2.140(3)	2.153(17)	2.1383(17)
Cu(1)−N(2)	2.117(3)	2.123(19)	2.1267(18)
Cu(1)−P(1)	2.2430(9)	2.2347(10)	2.2955(7)
Cu(1)−P(2)	2.2772(10)	2.2843(11)	2.2448(6)
N(1)−Cu(1)−N(2)	79.31(11)	79.3(4)	78.95(7)
N(1)−Cu(1)−P(1)	112.61(8)	115.6(8)	99.41(5)
N(2)−Cu(1)−P(2)	100.09(8)	101.2(9)	122.82(5)
P(1)−Cu(1)−P(2)	129.03(4)	127.40(4)	130.65(2)

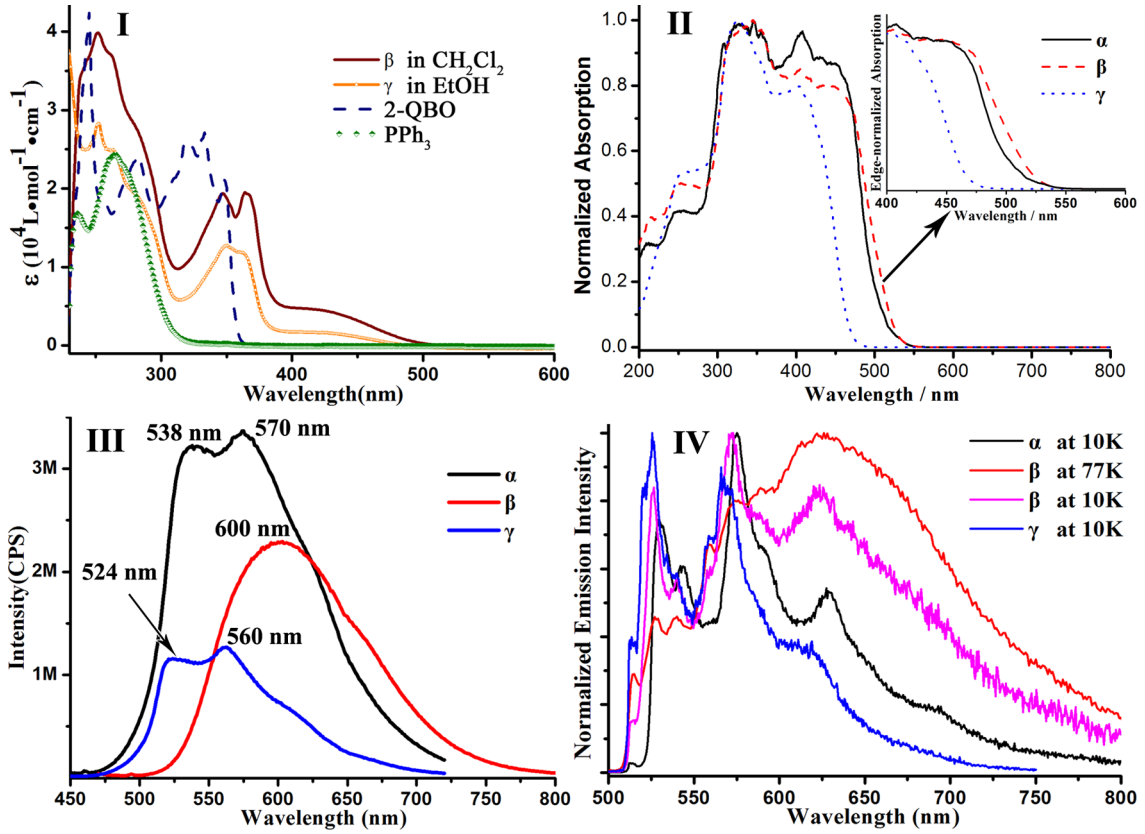

Figure 4. (I) UV−vis absorption spectra of the ligands and β in CH_2Cl_2 and γ in EtOH. (II) UV−vis diffuse reflection spectra for α, β, and γ powder samples. (III) Emission spectra of the three polymorphs in the solid state at room temperature (λ_{ex} = 365 nm). (IV) Comparison of emission spectra of the three polymorphs in the solid state at 10 K and β at 77 K.

DOI: 10.1021/ic502709b
Inorg. Chem. 2015, 54, 4200−4207

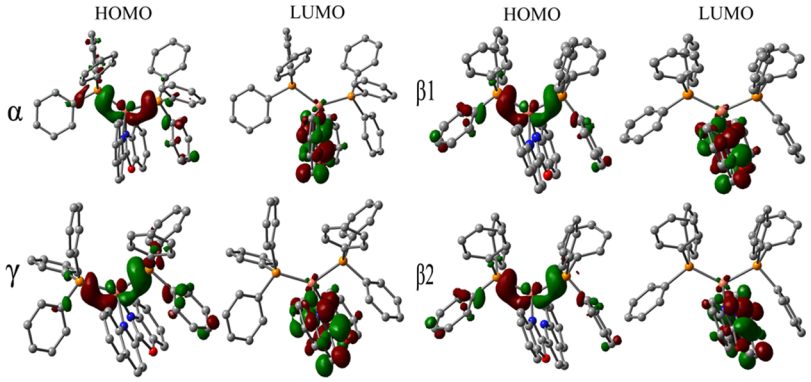

Figure 5. HOMOs and LUMOs frontier orbital plots of three polymorphs based on TD-DFT calculations. Isovalue = 0.05.

3.3. Spectroscopic Properties. *3.3.1. Spectroscopic Properties at Room Temperature.* It is found that α emits bright yellow light in the solid state at room temperature under UV (365 nm) irradiation, while β and γ emit orange and greenish-yellow light under the same irradiation, respectively (Figure 1). Thus, the interconversion of the polymorphs can also be easily distinguished by their emitting colors. The emission spectra of the three polymorphs were measured in the solid state at 298 K, and the absorption spectra of the free ligands, polymorphic β, and γ were measured in solution (Figure 4). Both ligands feature intense absorptions in the UV region, in which the lowest energy bands can be assigned as the $\pi-\pi^*$ transitions, centered at ∼265 and ∼330 nm for PPh_3 and 2-QBO, respectively.[18] Both of these bands locating at the high-energy region in the spectra of polymorphs can be attributed to the absorption of the ligands (Figure 4(I)). The lowest energy bands in β and γ show a maxima at ∼360 nm with an additional lower energy tail extending even to ∼500 nm. Because α is not soluble in a mixed EtOH/H_2O solvent, the diffuse reflection spectra of the three polymorphs have also been measured and compared, showing distinguished absorption onsets which agree well with their different crystal colors (Figure 4(II)).

As shown in Figure 4(III), the three polymorphs exhibit distinct luminescence behavior in the solid state. The emission spectra of α and γ are similar to a maxima near 570 and 560 nm and a shoulder at 538 and 524 nm, respectively. Obviously, vibronic structures are present in these spectra with spacings of 1050 and 1220 cm^{-1}, respectively, while β only exhibits a broad emission band (maxima at ∼600 nm) without any evident vibronic structure. This absence of vibronic structure in β can be attributed to its low emissive energy. It is well known that there are usually many vibronic states from different electronic energy levels in a molecule. In the case where the spacing of the two vibronic levels is large, a vibronic structure can be clearly observed just like in α and γ. In the case of β, however, the energy difference (emissive energy) is so small that no evident vibronic feature can be observed.

3.3.2. Low-Temperature Photoluminescent Properties. In order to further investigate the above vibronic structures, the PL spectra at 10 K were measured (Figure 4(IV)). Being different from the spectra at room temperature, the PL spectra at 10 K present two sharp peaks at 530 and 575 nm for α and 525 and 565 nm for γ. Besides these two main peaks, some satellite peaks can also be found at 543 and 592 nm for α and 513, 520, 534, 540, 558, and 572 nm for γ. In addition, two shoulders at 629 and 693 nm for α and one shoulder at 620 nm for γ can also be observed. Therefore, the vibronic structure in the room-temperature spectra of α and γ should be attributed to some vibronic energy levels of the complexes. It is of great interest that an obvious spectral variation is found in the PL spectrum of β when the temperature decreases from room temperature to 10 K. At 10 K, two sharp peaks at 525 and 570 nm with a shoulder at 620 nm are found in the spectrum, which is very similar to that of γ at 10 K, suggesting that β should have a phase transition at low temperature. For this reason, the PL spectrum of β was also measured at 77 K after the temperature was recovered from 10 K. As expected, a similar broad emission band is observed with comparison to its spectrum at room temperature. Close inspection of the spectrum shows that the maximum peak shifts from 600 to 620 nm, and some shoulders in the high-energy region are observed. Therefore, we proposed that β underwent a reversible phase transition to γ from 77 to 10 K. This conclusion is also consistent with the DFT calculations, in which γ is the most stable phase with a lower total energy of 0.2107 eV than that of β (Table 2).

3.4. Molecular Orbital Calculations. To further explore the excited states in these polymorphs, time-dependent DFT (TD-DFT) calculations at the B3LYP/LACVP* level of theory were performed on the X-ray structures.[8d] The frontier orbitals for the three polymorphs are shown in Figure 5, and other molecular orbitals related to the low-lying energy transition states (Supporting Information, Table S2) are shown in the Supporting Information, Figure S7−S9. In each polymorph, the LUMO orbital is delocalized over the π^* orbital of the 2-QBO ligand. Among them, the largest delocalization over 2-QBO in β than the others can be easily found. This orbital character directly leads to the lowest LUMO energy in β (Table 2), which is consistent with the best planarity of the 2-QBO ligand in β.[9] On the other hand, the HOMO in each polymorph is mainly a M−L antibonding orbital and shows its contribution from the Cu(I) d orbital and the P p orbital mixed with a little p orbital of phenyl group from the PPh_3 ligand. As shown in Table 2, the polymorphs present a sequence of $\beta > \alpha > \gamma$ in E_{HOMO}, which should be due to the smaller P−Cu−P angle ($\beta < \alpha < \gamma$) enlarging the energy of Cu−P σ antibonding orbitals, i.e., elevating the E_{HOMO}. Thus, the S1 and T1 excited states (HOMO → LUMO) can be assigned as (M + L′) → L charge transfer excited states, and their HOMO−LUMO gap energies ($\beta < \alpha < \gamma$, see Table 2) agree well with the lower energy emission/absorption bands. This is why those three polymorphs show different crystal color and PL properties. Actually, as shown in the Supporting Information, Table S2, all transitions from the H-n orbitals (under HOMO) to LUMO are similar to those associated with the HOMO → LUMO

DOI: 10.1021/ic502709b
Inorg. Chem. 2015, 54, 4200−4207

excited state (S_1 state). The calculated electronic absorption spectra that focus on low-lying energy transition singlet states are also shown in Figure 6, which is well in accordance with the experimental spectra (Figure 4(II)).

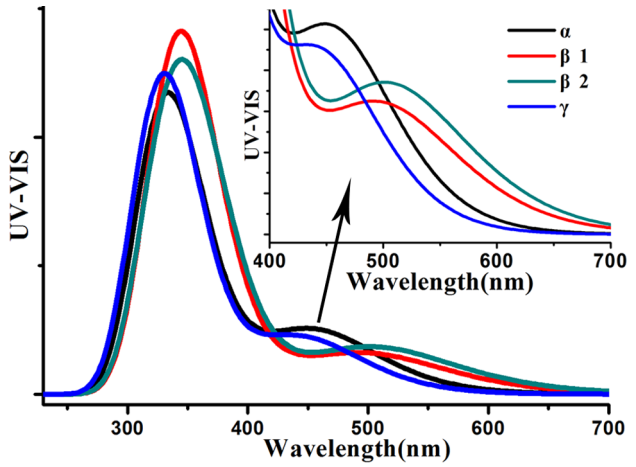

Figure 6. Calculated electronic absorption spectra of the three polymorphs focused on the low-lying energy transitions. (Inset) Absorption edges.

3.5. Thermogravimetric Analysis. The thermal stability of the three polymorphs, such as TG-DSC analyses, were performed on their powder samples (Figure 7). Just before

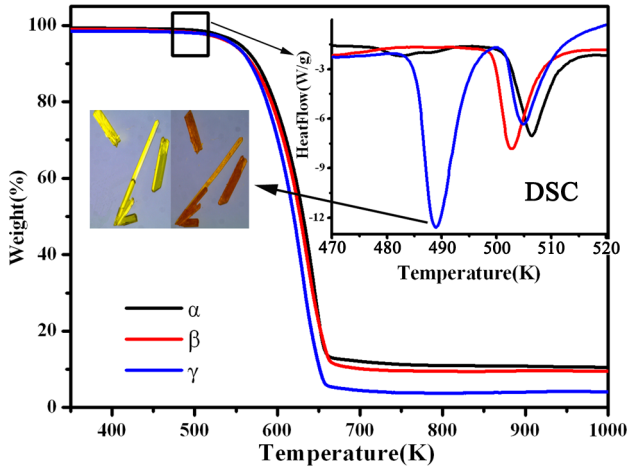

Figure 7. TG-DSC curves for the three polymorphs. The photograph clearly shows the phase transition from γ to β at ca. 490 K.

their decomposition, all polymorphs present a phase transition peak at ca. 503 K in the DSC curves, which has been proven as a melting process by a microscopic melting point test. Interestingly, an additional evident DSC peak can be observed for γ at ca. 490 K, and the heating experiment clearly indicates that this peak is attributed to a phase transition from γ to β (photograph in Figure 7). This is also consistent with the DFT calculations in which the value of E_T of β is larger than that of γ. Furthermore, this phase transition has been confirmed by the powder X-ray diffraction data (Figure 8). When γ was heated at 493 K for 5 min in air, the main phase has converted to β but some black matter was found on the surface of the sample probably due to the decomposition of the sample. Then the

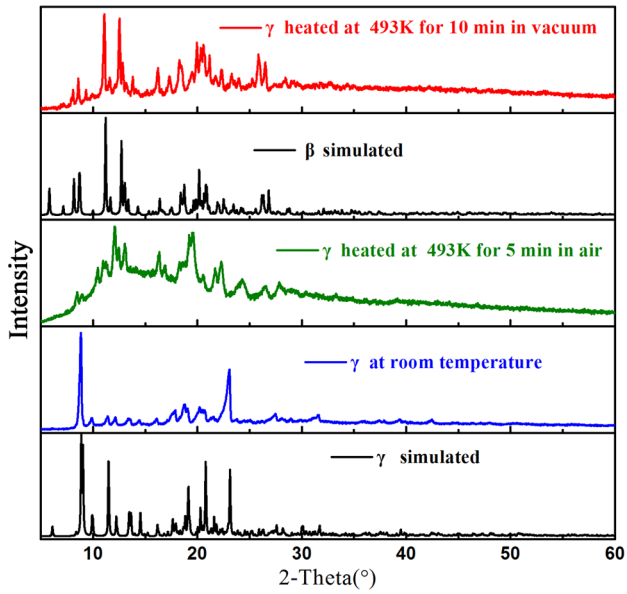

Figure 8. Powder XRD diffraction patterns, demonstrating the phase transition from γ to β at 493 K.

experimental condition was altered to heating at 493 K for 10 min in vacuum. Successfully, γ has all converted to β phase.

4. CONCLUSIONS

In summary, three polymorphs for copper(I) complex Cu(2-QBO)(PPh_3)PF_6 (**1**) triggered by the conformation isomerism of the ligand 2-QBO have been synthesized and characterized. The reversible conversions among these polymorphs have also been achieved at a certain temperature by using appropriate processing solvents based on their polarity variation. These polymorphs can be easily distinguished by the naked eye on the basis of their crystal morphologies and color under either natural light or PL character under UV light. The DFT/TD-DFT calculations reveal that E_T and μ are the two key factors associated with the polymorphic interconversion, and the magnitude of the θ value and P−Cu−P angle are the two key structural factors influencing the absorption and emission spectra.

■ ASSOCIATED CONTENT

Ⓢ Supporting Information

Crystallographic data in CIF format and some details for supramolecular structrures of the polymorphs α, β, and γ; CCDC 1025224−1025226 for α−γ; TD-DFT-calculated low-lying energy transitions, corresponding excited states, and MO diagrams of polymorphs α, β, and γ. This material is available free of charge via the Internet at http://pubs.acs.org.

■ AUTHOR INFORMATION

Corresponding Author

*E-mail: wxchai@cjlu.edu.cn.

Notes

The authors declare no competing financial interest.

■ ACKNOWLEDGMENTS

This research was supported by the Natural Science Foundation of Zhejiang Province (LY12E02010), the Foundation of State Key Laboratory of Structural Chemistry (20110011), the National Natural Science Foundation of

DOI: 10.1021/ic502709b
Inorg. Chem. 2015, 54, 4200−4207

China (61205184 and 11175169), and the Qianjiang Talents Project of Zhejiang Province (No. QJD1402028). X.C. acknowledges the partial support from the Special Project of National Major Scientific Equipment Development of China (No. 2012YQ120060).

■ REFERENCES

(1) Bernstein, J. *Polymorphism in Molecular Crystals*; Oxford: New York, 2002.
(2) Braga, D.; Grepioni, F. *Chem. Soc. Rev.* **2000**, *29* (4), 229−238.
(3) (a) Moulton, B.; Zaworotko, M. J. *Chem. Rev.* **2001**, *101* (6), 1629−1658. (b) Cruz-Cabeza, A. J.; Bernstein, J. *Chem. Rev.* **2013**, *114* (4), 2170−2191.
(4) Braga, D.; d'Agostino, S.; Dichiarante, E.; Maini, L.; Grepioni, F. *Chem.−Asian J.* **2011**, *6* (9), 2214−2223.
(5) (a) Colle, M.; Dinnebier, R. E.; Brutting, W. *Chem. Commun.* **2002**, *23*, 2908−2909. (b) Koshevoy, I. O.; Chang, Y.-C.; Karttunen, A. J.; Haukka, M.; Pakkanen, T.; Pi-Tai, C. *J. Am. Chem. Soc.* **2012**, *134* (15), 6564−6567. (c) Maini, L.; Braga, D.; Mazzeo, P. P.; Ventura, B. *Dalton Trans.* **2012**, *41* (2), 531−539. (d) Suzuki, T.; Yamaguchi, H.; Hashimoto, A.; Nozaki, K.; Doi, M.; Inazumi, N.; Ikeda, N.; Kawata, S.; Kojima, M.; Takagi, H. D. *Inorg. Chem.* **2011**, *50* (9), 3981−3987. (e) Mo, L. Q.; Jia, J. H.; Sun, L. j.; Wang, Q. M. *Chem. Commun.* **2012**, *48* (69), 8691−8693. (f) Kitagawa, H.; Ozawa, Y.; Toriumi, K. *Chem. Commun.* **2010**, *46* (34), 6302−6304. (g) Benito, Q.; Le Goff, X. F.; Maron, S.; Fargues, A.; Garcia, A.; Martineau, C.; Taulelle, F.; Kahlal, S.; Gacoin, T.; Boilot, J.-P.; Perruchas, S. *J. Am. Chem. Soc.* **2014**, *136* (32), 11311−11320.
(6) Tang, C. W.; Vanslyke, S. A. *Appl. Phys. Lett.* **1987**, *51* (12), 913−915.
(7) Rajeswaran, M.; Blanton, T. N.; Tang, C. W.; Lenhart, W. C.; Switalski, S. C.; Giesen, D. J.; Antalek, B. J.; Pawlik, T. D.; Kondakov, D. Y.; Zumbulyadis, N.; Young, R. H. *Polyhedron* **2009**, *28* (4), 835−843.
(8) (a) Moudam, O.; Kaeser, A.; Delavaux-Nicot, B.; Duhayon, C.; Holler, M.; Accorsi, G.; Armaroli, N.; Seguy, I.; Navarro, J.; Destruel, P.; Nierengarten, J. F. *Chem. Commun.* **2007**, *29*, 3077−3079. (b) Zhang, Q. S.; Zhou, Q. G.; Cheng, Y. X.; Wang, L. X.; Ma, D. G.; Jing, X. B.; Wang, F. S. *Adv. Mater.* **2004**, *16* (5), 432−436. (c) Zhang, Q. S.; Ding, J. Q.; Cheng, Y. X.; Wang, L. X.; Xie, Z. Y.; Jing, X. B.; Wang, F. S. *Adv. Funct. Mater.* **2007**, *17* (15), 2983−2990. (d) Zhang, X.; Song, L.; Hong, M.; Shi, H.; Xu, K.; Lin, Q.; Zhao, Y.; Tian, Y.; Sun, J.; Shu, K.; Chai, W. *Polyhedron* **2014**, *81* (0), 687−694. (e) Bergmann, L.; Friedrichs, J.; Mydlak, M.; Baumann, T.; Nieger, M.; Braese, S. *Chem. Commun.* **2013**, *49* (58), 6501−6503.
(9) Klyuev, N. A.; Kurapov, P. B.; Aleksandrov, G. G.; Grandberg, I. I. *Chem. Heterocycl. Compd.* **1982**, *18* (6), 585−589.
(10) Sheldrick, G. *Acta Crystallogr., Sect. A* **2008**, *64* (1), 112−122.
(11) Frisch, M.J.; G. W. T, Schlegel, H.B.; Scuseria, G.E.; Robb, M.A.; Cheeseman, J.R.; Scalmani, G.; Barone, V.; Mennucci, B.; Petersson, G.A.; Nakatsuji, H.; Caricato, M.; Li, X.; Hratchian, H.P.; Izmaylov, A.F.; Bloino, J.; Zheng, G.; Sonnenberg, J.L.; Hada, M.; Ehara, M.; Toyota, K.; Fukuda, R.; Hasegawa, J.; Ishida, M.; Nakajima, T.; Honda, Y.; Kitao, O.; Nakai, H.; Vreven, T.; J. A. Jr. Montgomery, Peralta, J.E.; Ogliaro, F.; Bearpark, M.; Heyd, J.J.; Brothers, E.; Kudin, K.N.; Staroverov, V.N.; Kobayashi, R.; Normand, J.; Raghavachari, K.; Rendell, A.; Burant, J.C.; Iyengar, S.S.; Tomasi, J.; Cossi, M.; Rega, N.; Millam, J.M.; Klene, M.; Knox, J.E.; Cross, J.B.; Bakken, V.; Adamo, C.; Jaramillo, J.; Gomperts, R.; Stratmann, R.E.; Yazyev, O.; Austin, A.J.; Cammi, R.; Pomelli, C.; Ochterski, J.W.; Martin, R.L.; Morokuma, K.; Zakrzewski, V.G.; Voth, G.A.; Salvador, P.; Dannenberg, J.J.; Dapprich, S.; Daniels, A.D.; Farkas, O.; Foresman, J.B.; Ortiz, J.V.; Cioslowski, J.; Fox, D.J.; Wallingford, C.T. *Gaussian 09*; Gaussian, Inc.: Wallingford, CT, 2009.
(12) Allesø, M.; van den Berg, F.; Cornett, C.; Jørgensen, F. S.; Halling-Sørensen, B.; de Diego, H. L.; Hovgaard, L.; Aaltonen, J.; Rantanen, J. *J. Pharm. Sci.* **2008**, *97* (6), 2145−2159.
(13) Reichardt, C.; Welton, T. Empirical Parameters of Solvent Polarity. In *Solvents and Solvent Effects in Organic Chemistry*; Wiley-VCH Verlag GmbH & Co. KGaA: New York, 2010; pp 425−508.
(14) Armaroli, N.; Accorsi, G.; Cardinali, F.; Listorti, A. Photochemistry and Photophysics of Coordination Compounds: Copper. In *Photochemistry and Photophysics of Coordination Compounds*; Balzani, V., Campagna, S., Eds.; Springer: Berlin Heidelberg, 2007; Vol. *280*, pp 69−115.
(15) Liu, X.; Sun, W.; Zou, L.; Xie, Z.; Li, X.; Lu, C.; Wang, L.; Cheng, Y. *Dalton Trans.* **2012**, *41* (4), 1312−1319.
(16) (a) Chai, W.-X.; Lin, J.; Song, L.; Qin, L.-S.; Shi, H.-S.; Guo, J.-Y.; Shu, K.-Y. *Solid State Sci.* **2012**, *14* (8), 1226−1232. (b) Chai, W.-X.; Song, L.; Lin, J.; Shu, K.-Y.; Qin, L.-s.; Shi, H.-s.; Guo, J.-Y. *J. Inorg. Organomet. Polym.* **2012**, *22* (6), 1263−1270.
(17) Chai, W.; Lin, J.; Song, L.; Shu, K.; Qin, L.; Shi, H.; Guo, J. *Solid State Sci.* **2010**, *12* (12), 2100−2105.
(18) Xu, K.; Hong, M.; Zhang, Y.; Song, L.; Chai, W. *Acta Crystallogr., Sect. C* **2014**, *70* (Pt 9), 858−61.

DOI: 10.1021/ic502709b
Inorg. Chem. 2015, 54, 4200−4207